Performance Assessment of Cross-Directional Control for Paper Machines

Qiugang Lu, Michael G. Forbes, R. Bhushan Gopaluni, Philip D. Loewen, Johan Backstrom, and Guy A. Dumont

***Abstract*—The minimum variance controller (MVC) has been extensively used as a benchmark in the performance assessment of both univariate and multivariate control loops when the time-delay is the fundamental performance limitation. In this paper, the spatial and temporal performance limitations in the cross-directional (CD) control of paper machines are analyzed. The idea of minimum variance benchmarking is extended to the CD process based on these performance limitations. Based on an industrial CD controller, a user-specified benchmark, which is more practical and less aggressive, is also proposed. In addition, several related performance indices are proposed for the CD process based on both the minimum variance benchmark and the user-specified benchmark. Illustrative examples from a paper machine simulator and industrial data sets are provided to show the effectiveness of the proposed performance indices.**

***Index Terms*—Performance assessment, minimum variance benchmark, cross-direction processes, paper machine.**

I. Introduction

THE function of a paper machine is to efficiently transform a slurry of water and wood cellulose fibers into sheets of paper. The array of actuators at the headbox across the paper sheet is used to adjust the properties of the pulp distributed across the paper sheet, and the array of sensors located at the end of paper machine will measure the properties such as ***basis weight, moisture, and thickness***. A schematic of a typical paper machine is illustrated in Figure 1. The goal is to make the measured paper properties as close to desired as possible by adjusting the actuators.

In the literature, the direction in which the paper sheet travels is defined as machine direction (MD) and the direction perpendicular to the sheet travel is defined as the cross direction (CD), as shown in Figure 1. Compared with MD control, CD control is much more complex due to the characteristics associated with the CD processes [1], [2]. First,

Qiugang Lu is with the Department of Chemical and Biological Engineering, The University of British Columbia, Vancouver, BC, Canada. E-mail: qglu@chbe.ubc.ca

Michael Forbes is with Honeywell Process Solutions, 500 Brooksbank Ave, North Vancouver, BC, Canada. E-mail: michael.forbes@honeywell.com

Bhushan Gopaluni is with the Department of Chemical and Biological Engineering, The University of British Columbia, Vancouver, BC, Canada. E-mail: bhushan.gopaluni@ubc.ca

Philip Loewen is with the Department of Mathematics, The University of British Columbia, Vancouver, BC, Canada. E-mail: loew@math.ubc.ca

Johan Backstrom is with Honeywell Process Solutions, 500 Brooksbank Ave, North Vancouver, BC, Canada. E-mail: johan.backstrom@honeywell.com

Guy Dumont is with the Department of Electrical and Computer Engineering, The University of British Columbia, Vancouver, BC, Canada. E-mail: guyd@ece.ubc.ca

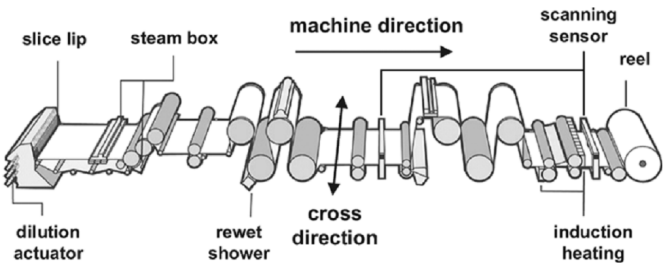

Fig. 1. The structure of a typical industrial paper machine with arrays of actuators and sensors [29].

a typical industrial paper machine may be as wide as 10 meters with hundreds of actuator and measurement bins. If modeled as a multivariable system, the huge dimension will make the controller design a challenging problem [3]. Second, ***due to the spatially-distributed nature of the CD process, most CD process models are often ill-conditioned, and consequently, a large portion of the eigenvector directions with small eigenvalues are indeed uncontrollable [4]***. Third, the model uncertainty and the gain sign uncertainty associated with the uncontrollable ***eigenvector*** directions make robust stability especially difficult to achieve [5], [6]. So far, most CD controllers are based on a model identified *a priori* from experiments such as bump tests [7], [8]. Classical CD control strategies include two dimensional loop shaping [28], CD model predictive control ***(MPC)*** [38], and robust CD control [9]. In these conventional CD control techniques, the quality of the CD process model plays a vital role in determining the closed-loop performance of control loops. However, as the process operating conditions change [39], the quality of the CD process model may deteriorate and consequently the control performance will degrade. As a result, a new model must be identified for the CD process. Therefore, it is desirable to develop techniques to monitor the performance of CD controllers using routine operating data.

When it comes to performance monitoring, a variety of approaches have emerged since Harris first proposed using the minimum variance controller (MVC) as a performance benchmark [10]. The MVC benchmark is widespread since it represents the minimum variance that a closed-loop system can achieve when the time-delay is the fundamental performance limitation. A time series model has to be fitted into the measured output data and the first few coefficients are the controller-invariant part (benchmark). The filtering and correlating (FCOR) algorithm is proposed in [14] in which only

the output measurements and the time delay are required to calculate the minimum variance benchmark. Furthermore, the MVC benchmark is extended from single-input single-output (SISO) systems to multiple-input multiple-output (MIMO) systems [11]–[13]. Note that for MIMO systems, the interactor matrix has to be factored out as an analogy of the time-delay for the SISO case in order to apply the MVC benchmark. Moreover, it has been proved that the multivariate MVC is able to achieve minimum variance in each individual output channel provided the interactor matrix is simple or diagonal [14]. However, most MIMO systems under investigation in performance monitoring are well conditioned with small input and output dimensions. A suitable extension of MVC benchmarking to the spatially distributed system, such as the cross-direction of paper machines, has received relatively little attention. ***The high dimensionality of measurements as well as the poorly conditioned nature of the CD process model presents significant challenges for performance monitoring [39]***.

Nevertheless, in practice, most controllers implemented in industrial processes differ from MVC due to the poor stability margin and excessive actuation effort associated with achieving minimum variance. Therefore, more practical performance monitoring benchmarks have been developed, such as generalized MVC benchmark [31], linear quadratic control (LQG) benchmark [14], model predictive control benchmark [24], [32]–[34], user-specified benchmark [14], [15], etc. A user-specified benchmark accounts for the practical situation where the measured output variance is compared with a user-specified target (can be defined based on the knowledge of actual implemented controller) instead of a theoretical minimum.

So far there have been few articles focusing on the performance assessment of CD processes. In [18], the deviation of an implemented controller from the MVC is estimated in terms of actual input-output data as well as the plant model (known *a priori*). More practical considerations such as actuator constraints are taken into account in the monitoring process. In [19], the original CD model is decoupled into a family of SISO systems and Harris' MVC benchmark is applied to each mode. More recently, the minimum variance performance index for CD processes is proposed in [17] which accounts for both time-delay performance limitations in the temporal direction and spatial bandwidth performance limitations in the spatial direction. A Bayesian method is employed in order to apply a Toeplitz structure to the coefficient matrices for estimation in the time series model. However, it is not straightforward to obtain a quantitative assessment of the CD processes from the proposed methods. Thus it is desirable to develop an intuitive performance index which directly measures the control performance for the CD process. Moreover, the performance index must be reasonably easy to compute so as to implement it on-line.

However, control loop performance may deteriorate for various reasons such as model-plant mismatch (poor quality model), the change of disturbance characteristics, improper tuning of controllers, etc. [32]. Among these factors the model-plant mismatch (MPM) is vital since when the mismatch degrades the control performance, system re-identification will be required to produce an updated model and deploy it in the controller. Note that it is not necessary to do model re-identification for the other causes of performance degradation. As system identification experiments are generally quite expensive and time-consuming [40], the sensitivity of the benchmark or performance index with respect to the model-plant mismatch will be extremely important. An ideal performance index would be an intuitive and reliable indicator sensitive to mismatch, showing the current performance of control systems. The engineers or automatic supervision systems can make decisions as to whether further maintenance is necessary based on this index. So far there have been several papers investigating the effect on various performance indices caused by MPM [16], [20]–[22]. However, for the CD process, there is no relevant literature focusing on the relation between performance indices and MPM. It is worth pointing out that the most desirable case is to find ***a*** benchmark which is merely sensitive to the model-plant mismatch while robust to other factors such as disturbance model changes.

The objective of this paper is to propose performance indices based on both MVC benchmark and user-specified benchmark for the CD process, such that the MVC benchmark accounts for both the temporal and spatial performance limitation. The performance index is expected to be sensitive to MPM but insensitive to the spatial disturbances. The background knowledge on the variance partition and the process model of the CD process are presented in Section II. In Section III, the MVC benchmark for the steady-state profile and the residual profile are derived. New performance indices based on the MVC benchmark are proposed afterwards. Furthermore, the MVC benchmarks are extended to the user-specified benchmark in Section IV. A novel algorithm is developed in Section V which significantly reduces the computational complexity in the multivariate time series model estimation. Finally, illustrative examples are provided to validate the effectiveness of the proposed benchmarks. As the intended use of the performance index is to reflect the quality of the model used by the controller, it is desirable that the performance index is insensitive to the spatial high-frequency disturbances to avoid the drop of the performance index caused by the disturbances. The sensitivity of proposed performance indices to high frequency spatial disturbances is also analyzed in this section.

II. Preliminaries

In this section, a preliminary introduction to the commonly used variance partition technique for the CD data set is provided. The dynamic model and steady-state model for the CD process are presented afterwards.

A. Variance Partition

A given data set $Y \in \mathbb{R}^{m\times N}$ from a paper machine can always be separated into machine-direction (MD), cross-direction and residual components, where m is the number of measurement bins, and N is the number of scans in the data set. For details on the calculation and partitioning of variance, see the Appendix A. In terms of CD control and CD performance

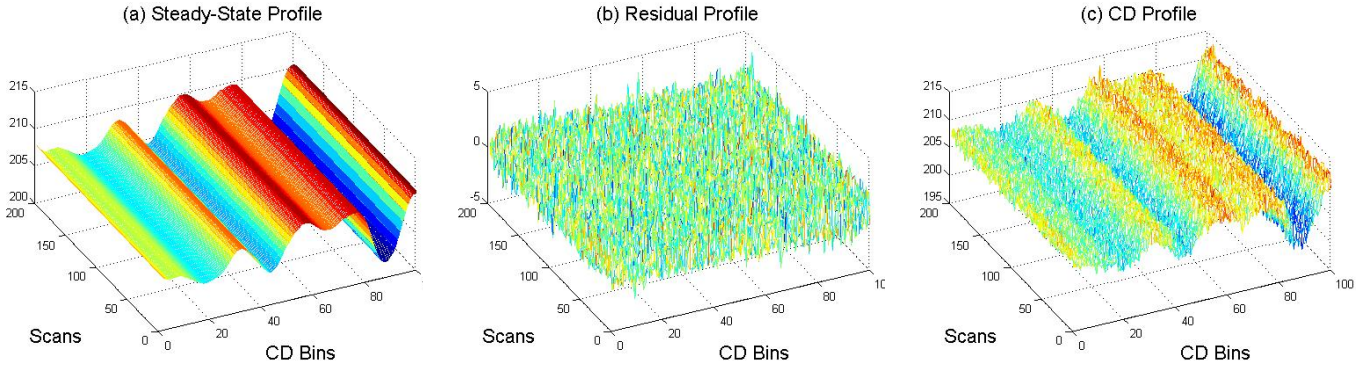

Fig. 2. Illustration of the variation separation. (a): The steady-state profile plot. Note that the steady-state profile is replicated to have the same scan number as the residual profile and CD profile; (b): The residual profile plot. Each CD bin has zero mean; (c): The overall CD profile. Note that the CD profile is combined by the steady-state and the residual profile.

monitoring, the MD variation is not taken into account. The data set without MD variation at time t is denoted as $y(t) \in \mathbb{R}^m$ (CD profile), and we have

$$y(t) = y_{ss} + y_r(t), \tag{1}$$

where $y_{ss} \in \mathbb{R}^m$ is the steady-state profile, which is constant over all scans. $y_r(t) \in \mathbb{R}^m$ is the residual profile and is changing over time. Figure 2 shows the graphs of the steady-state profile, the residual profile and the CD profile. The process models for the steady-state profile and the residual profile will be given in the following subsection, and the motivation to treat them separately will be presented in Section V.

B. Process Model

In the traditional CD control, the steady-state performance is of great importance since most paper machines are working in the regulatory mode at steady-state. The static steady-state model of the CD process is expressed as,

$$y_{ss} = Gu_{ss} + v_{ss}, \tag{2}$$

where $y_{ss} \in \mathbb{R}^m$ ***is the steady-state controlled variable and*** m ***is the number of data boxes.*** $u_{ss} \in \mathbb{R}^n$ ***is the steady-state manipulated variable, where*** n ***is the number of actuator zones. For typical paper machines, we usually have*** $m >> n$ ***and*** m ***is an integer multiple of*** n***.*** $G \in \mathbb{R}^{m\times n}$ ***is the steady-state gain matrix and each column of*** G ***describes the sampled spatial impulse response of a single actuator. Typically,*** G ***is poorly conditioned and non-square with several times more rows than columns.*** v_{ss} ***is the steady-state disturbance which refers to a deterministic disturbance persistently acting on the output, e.g., a spatial sinusoidal disturbance which is not changing over time. For the CD process, the overall disturbance is assumed to be a combination of the steady-state disturbance*** v_{ss} ***and a filtered white noise*** $v_r(t)$***, which will be explained in*** (3)***.***

When considering only the residual profile, we will have the following model,

$$y_r(t) = g(z^{-1})Gu_r(t) + v_r(t), \tag{3}$$

where $y_r(t) = y(t) - y_{ss}$ can be considered as the deviation of the process output from the steady-state value due to the stochastic disturbances. Similarly, $u_r(t) = u(t) - u_{ss}, v_r(t) = v(t) - v_{ss}$ are the deviations of the manipulated variable and disturbance from their steady-state values, ***respectively***. $g(z^{-1})$ is usually a scalar transfer function representing the temporal dynamics of the CD process. The variable z^{-1} represents the unit back-shift operator. The output disturbance, $v_r(t) \in \mathbb{R}^m$, is generally assumed to be filtered white noise. Note that the subscripts r in (3) stand for the residual.

The scalar transfer function $g(z^{-1})$ in (3) can further be expressed as,

$$g(z^{-1}) = z^{-d}\frac{B(z^{-1})}{A(z^{-1})}, \tag{4}$$

where d stands for the time-delay and $B(z^{-1})$ and $A(z^{-1})$ are scalar polynomials. Typically, the temporal model of the CD process is assumed to be first order plus time-delay with unit steady-state gain. Similarly, the stochastic disturbance $v_r(t)$ in (3), is filtered white noise assumed to be temporally and spatially separable, denoted as,

$$v_r(t) = \frac{C(z^{-1})}{A(z^{-1})}\phi e(t), \tag{5}$$

where $C(z^{-1})$ and $A(z^{-1})$ are scalar polynomials describing the temporal filter while the constant matrix, ϕ, is used to represent the spatial filtering of the white noise vector $e(t)$. The covariance matrix of the white noise vector $e(t)$ is assumed to be $\mathbb{E}[e(t)e^T(t_0)] = \Sigma_e\delta(t-t_0)$, where $\mathbb{E}$ is the expectation operator, Σ_e is the covariance matrix and δ is the Dirac delta function.

Remark 1: From the above description on the steady-state and residual profiles, one is able to interpret each entry of the steady-state profile y_{ss} as the mean of the corresponding output channel (measurement bin). Each entry of the residual profile $y_r(t)$ is the deviation of the profile from the corresponding mean value.

III. The MVC Benchmark for CD Processes

In this section, the performance limitations for both the steady-state model (2) and the residual dynamic model (3) are illustrated. The MVC benchmarks for both models are developed analogously, and new performance indices are proposed based on these benchmarks.

A. MVC Benchmark for the Steady-State Profile

For the steady-state model (2), the optimal control input u_{ss} which minimizes the output variance has the structure,

$$u_{ss} = -(G^T G)^{-1} G^T v_{ss}, \tag{6}$$

which is exactly the pseudo-inverse of G matrix. It has been proved in [35] that if the controller has the structure (6) and an integrator in the dynamic part, then the steady-state output profile y_{ss} will contain no components in the column space of G, which is regarded as the controllable subspace. If G matrix is square and invertible, then the optimal input is able to achieve zero steady-state output. Therefore, the structure of G matrix limits the performance for the steady-state model (2). For non-square G matrix with full rank, i.e., $rank\{G\} = \min\{m,n\}$, the output y_{ss} with minimal variance is,

$$y_{ss} = [I - G(G^T G)^{-1} G^T] v_{ss}. \tag{7}$$

In order to demonstrate the controller form which is able to achieve the minimal steady-state variance, we assume that the controller $K(z^{-1})$ has the following structure (refer to [35]),

$$K(z^{-1}) = k(z^{-1})(G^T G)^{-1} G^T. \tag{8}$$

where $k(z^{-1})$ is the scalar dynamic part of $K(z^{-1})$. From (8), the closed-loop sensitivity function is obtained as,

$$y(t) = [1 + g(z^{-1}) G K(z^{-1})]^{-1} v(t). \tag{9}$$

From singular value decomposition (SVD) of G, (9) is further simplified as,

$$\begin{bmatrix} y_c(t) \\ y_u(t) \end{bmatrix} = \begin{bmatrix} \frac{1}{1+g(z^{-1})k(z^{-1})} & 0 \\ 0 & I_{(m-n)\times(m-n)} \end{bmatrix} \begin{bmatrix} v_c(t) \\ v_u(t) \end{bmatrix}, \tag{10}$$

where the subscripts c and u refer to spatially controllable and spatially uncontrollable signals, respectively. If $k(z^{-1})$ has an integrator, at steady-state, (10) will become,

$$\begin{bmatrix} y_{ss,c} \\ y_{ss,u} \end{bmatrix} = \begin{bmatrix} 0 & 0 \\ 0 & I_{(m-n)\times(m-n)} \end{bmatrix} \begin{bmatrix} v_{ss,c} \\ v_{ss,u} \end{bmatrix}. \tag{11}$$

It is clear that the MVC for the steady-state model (2) will completely remove all disturbance components within the controllable subspace. However, those disturbance components within the uncontrollable subspace will not be affected by the controller. Therefore, the spatially uncontrollable components $y_{ss,u}$ can be used as a benchmark for the MVC. Note that the actual steady-state profile under a CD controller such as CD-MPC (not spatial MVC) may have components left in the controllable subspace.

B. MVC Benchmark for the Residual Profile

For the residual profile, in the spatial direction, as with the steady-state case, due to there being more CD bins than actuator zones, i.e., G is not square, not all of the directions of the transfer matrix G are controllable. This means that it is impossible to design a controller to reach zero error for a given disturbance. Therefore, the structure of the G matrix contributes to the spatial performance limitation in the CD controller. In addition to the spatial performance limitation, the residual profile (3) also suffers temporal performance limitation due to the dynamics. In the temporal direction, the time-delay forms the fundamental limitation on the controller design, upon which various types of delay compensators arise such as dead-beat controller, minimum variance controller, Dahlin controller, etc.

For the disturbance model (5), from the Diophantine identity, we have

$$\frac{C(z^{-1})}{A(z^{-1})} = F(z^{-1}) + z^{-d}\frac{H(z^{-1})}{A(z^{-1})}, \tag{12}$$

where $F(z^{-1})$ and $H(z^{-1})$ are scalar polynomials, i.e.,

$$F(z^{-1}) = f_0 + f_1 z^{-1} + \ldots + f_{d-1} z^{-d+1}, \tag{13}$$

$$H(z^{-1}) = h_0 + h_1 z^{-1} + \ldots + h_{n_h} z^{-n_h}. \tag{14}$$

Considering the profile at time $t+d$ (supposing the current time is t), from (12) we have

$$y_r(t+d|t) = \hat{y}_r(t+d|t) + F(z^{-1})\phi e(t+d), \tag{15}$$

where $\hat{y}_r(t+d|t)$ represents the d-step-ahead prediction [23] at t, namely,

$$\hat{y}_r(t+d|t) = \frac{B(z^{-1})F(z^{-1})}{C(z^{-1})} G u_r(t) + \frac{H(z^{-1})}{C(z^{-1})} y_r(t). \tag{16}$$

Note that the second term in (15) is the unpredictable future profile due to the time delay, which is controller invariant. The first term of (15) is controller-dependent and by minimizing $\mathbb{E}[\hat{y}_r(t+d|t)\hat{y}_r^T(t+d|t)]$ we will achieve the minimum variance of the residual profile. If the transfer matrix G in (16) is square and invertible, it is possible to find an input sequence such that $\hat{y}_r(t+d|t) = 0$. However, due to the special structure, G is often non-square, and hence the minimum variance of $\hat{y}_r(t+d|t)$ is achieved by setting

$$u_r(t) = -G^{\dagger}\frac{H(z^{-1})}{B(z^{-1})F(z^{-1})} y_r(t), \tag{17}$$

where $G^{\dagger} = (G^T G)^{-1} G^T$ is the pseudo-inverse of G. It should be noted that $G^{\dagger}$ indeed represents the MVC in the spatial direction due to the special structure of G (refer to (6) and (11)) while $\frac{H(z^{-1})}{B(z^{-1})F(z^{-1})}$ denotes the temporal MVC due to time delay. Therefore, (17) stands for the temporal and spatial MVC for the residual model (3).

Based on previous observations, the profile at $t+d$ in (15) can be further decomposed as,

$$y_r(t+d|t) = \hat{y}_{r,c}(t+d|t) + \underbrace{\hat{y}_{r,u}(t+d|t) + F(z^{-1})\phi e(t+d)}_{\text{controller-invariant}}, \tag{18}$$

where the subscript c stands for spatially controllable, and the subscript u refers to spatially uncontrollable part of $y_r(t+d|t)$, where the controllable subspace is defined as the column space of G, as for the steady-state case. It can be observed in (18) that the last two terms are the controller-invariant, both spatially and temporally, parts of the profile, and hence can be used to define a benchmark for performance assessment. If the current controller being implemented is MVC, then the first term on the right hand side of (18) disappears.

C. New Performance Indices

Based on the proposed MVC benchmarks for both the steady-state profile and the residual profile in (7) and (18), a new MVC performance index for the CD process can be defined as

$$\eta_1 = \frac{trace\left[\sum_{i=0}^{d-1} F_i \Sigma_e F_i^T + \Sigma_{\hat{y}_{r,u}} + diag(y_{ss,u} y_{ss,u}^T)\right]}{trace\left(\Sigma_{y,mse}\right)}, \quad (19)$$

where $F_i = f_i \phi$, $\Sigma_{\hat{y}_{r,u}}$ is the covariance matrix of the uncontrollable predicted profile $\hat{y}_{r,u}$, and $diag(\cdot)$ is a matrix formed by the diagonal elements. For instance,

$$X = \begin{bmatrix} x_1 & x_2 \\ x_3 & x_4 \end{bmatrix}, \quad diag(X) = \begin{bmatrix} x_1 & 0 \\ 0 & x_4 \end{bmatrix}.$$

The term in the denominator $\Sigma_{y,mse}$ is defined as,

$$\Sigma_{y,mse} = \Sigma_{y_r} + diag(y_{ss} y_{ss}^T), \quad (20)$$

where Σ_{y_r} is the covariance matrix of the residual profile, each element on the diagonal represents the variance of an individual output channel of y_r. For the term $diag(y_{ss} y_{ss}^T)$, each element stands for the corresponding mean deviation from zero of each individual output channel. In (19), the first term of the numerator $\sum_{i=0}^{d-1} F_i \Sigma_e F_i^T$ represents the covariance of unpredictable components in the residual profile. The second term $\Sigma_{\hat{y}_{r,u}}$ indicates the covariance of the spatially uncontrollable predicted residual profile. The third term $diag(y_{ss} y_{ss}^T)$ stands for the spatially uncontrollable portion of the steady-state profile. Thus the numerator of (19) specifies the measure of both the residual MVC benchmark (18) and the steady-state MVC benchmark (7). On the other hand, the denominator of (19) represents the overall mean square error (MSE) of the output profile. Hence, the new MVC performance index η_1 is the ratio between the covariance of the benchmark of $y(t)$ and its total variance (see Appendix A). If the implemented controller is the MVC, the index η_1 will be equal to one as the measured output y only contains the uncontrollable components, which are exactly the terms shown in the denominator of (19). Otherwise, η_1 will be less than one and smaller value of η_1 implies worse control performance.

From the performance index in (19), we can see that one has to separate the spatially uncontrollable components $\hat{y}_u(t)$ from $\hat{y}(t)$ in (18) in order to evaluate the benchmark. Besides, this performance index takes the spatially uncontrollable components into account. In industrial CD control systems, ***the spatially uncontrollable components of the disturbances*** almost remain untouched. Therefore, we expect the performance index (19) to be sensitive to high-frequency spatial disturbances. If there is a great amount of spatially high-frequency disturbances (beyond the spatial bandwidth) coming in, the performance index (19) will be inflated by these high-frequency components, and therefore the performance index will be always close to one (this will be illustrated in the simulation part). In this case, the performance index η_1 becomes incapable of detecting the performance drop. An alternative is to separate the white noise $e(t)$ into spatially uncontrollable components $e_u(t)$ and controllable components $e_c(t)$, then (18) can be rewritten as,

$$\begin{aligned} y_r(t+d|t) &= \hat{y}_{r,c}(t+d|t) + F(z^{-1})\phi e_c(t+d) \\ &\quad + \underbrace{F(z^{-1})\phi e_u(t+d) + \hat{y}_{r,u}(t+d|t)}_{y_{r,u}(t+d|t)}, \end{aligned} \quad (21)$$

where $F(z^{-1})\phi e_u(t+d|t)$ and $\hat{y}_{r,u}(t+d|t)$ are combined as $y_{r,u}(t+d|t)$, the uncontrollable parts of $y_r(t+d|t)$. Specifically, define the projection operators $\mathbb{P}_c$ and $\mathbb{P}_u$ which project the profile into the spatially controllable and uncontrollable subspaces, respectively. For the column space framework, $\mathbb{P}_c$ and $\mathbb{P}_u$ are defined as,

$$\mathbb{P}_c = (G^T G)^{-1} G^T, \quad \mathbb{P}_u = I - (G^T G)^{-1} G^T. \quad (22)$$

Then we have,

$$y_{r,u}(t+d|t) = \mathbb{P}_u y_r(t+d|t), \quad y_{ss,u} = \mathbb{P}_u y_{ss}. \quad (23)$$

From (23) one can see that the spatially uncontrollable components of both the steady-state profile and the residual profile can be extracted by using the operator $\mathbb{P}_u$. In order to solve the problem with the performance index (19) being sensitive to spatially high-frequency disturbances, the following modified performance index is suggested,

$$\eta_2 = \frac{trace\left[\sum_{i=0}^{d-1} F_i \Sigma_{e_c} F_i^T\right]}{trace(\Sigma_{y_{c,mse}})}, \quad (24)$$

where $\Sigma_{e_c} = \mathbb{E}[e_c e_c^T]$ is the covariance matrix of the white noise within the spatially controllable subspace. The covariance matrix in the denominator is further expressed to be,

$$\Sigma_{y_{c,mse}} = \Sigma_{y_{r,c}} + diag(y_{ss,c} y_{ss,c}^T), \quad (25)$$

where $\Sigma_{y_{r,c}}$ is the covariance matrix of the spatially controllable residual profile. The performance index (24) compares the covariance of the unpredictable disturbance within the controllable subspace with the mean square error of the controllable output profile. This performance index is not sensitive to high-frequency spatial disturbances since the spatially uncontrollable components have been removed before calculating the performance index.

Remark 2: Note that the numerator of (24) includes only the residual part, which makes sense since if the implemented controller has the spatial MVC structure (6) and an integrator, then the components of the steady-state profile within the controllable subspace (the steady-state benchmark) will be zero. However, since most implemented controllers are not MVC, there will be components left in the spatially controllable subspace, which explains the steady-state terms in (25).

Remark 3: The motivation of modifying performance index η_1 into η_2 is as follows. If large spatial steady-state disturbance is present in the output, e.g., spatial sinusoidal disturbance with frequency beyond the spatial bandwidth, both the numerator and the denominator of η_1 will be inflated. Consequently, η_1 will be unable to assess the controller performance as it will be always close to one, independent of whether the controller is performing well

or not. For η_2, the spatially uncontrollable components are removed from the steady-state profile and the residual profile. In other words, η_2 is indeed comparing the spatially controllable, temporally uncontrollable residual profile with the overall spatially controllable output profile. As a result, the peformance index η_2 will be able to reflect the performance of the controller even with the presence of large high-frequency steady-state disturbances.

IV. User-Specified Benchmark

It has been well known that for control loops MVC requires aggressive control actions and lacks robustness to model uncertainties. Consequently, MVC is not widely used in the process industry. ***In practice, to guarantee the robust stability and performance, the implemented controllers are much more sluggish than the MVC. If the MVC is still used as the benchmark, then most industrial controllers will show very low performance index even though the underlying control loop is indeed operating with satisfactory performance. In such cases, the observation of low performance index based on MVC benchmark does not necessarily imply poor controller design. Therefore, it is important to develop practical benchmarks based on the specific controller that is implemented on the process.*** The user-specified benchmark is the outcome of this idea, where a filter is defined as the desired closed-loop behavior and a parameter in the filter can be tuned to change the aggressiveness and conservativeness of the benchmark. In this section, the user-specified benchmark will be adapted to the CD process to make our benchmark more realistic.

For the CD process, we note that the spatial part of the MVC, $G^{\dagger}$ in (17), removes the components of the disturbance profile within the subspace spanned by the columns of G. However, due to the spatially-distributed nature, the G matrix for most CD processes has a large condition number. The ill-conditioned property of G implies that some of the singular values are vanishingly small. Therefore, the corresponding singular vector directions are considered uncontrollable and avoided in the CD controller so as to ensure robust stability and acceptable actuator action. It is therefore more realistic to select those (pseudo) singular vector directions (or spatial frequencies from the perspective of the Fourier matrix transform) with significant mode gains and without wrong signs as controllable directions [36], which typically corresponds to the low spatial frequency range (specified by spatial bandwidth in this paper).

The selection of the desired spatial benchmark is not fixed depending on the specific CD controller that is being used. For instance, if we are using CD MPC, we may choose a spatial frequency dependent sensitivity function as the benchmark, which can be obtained from the steady-state weighting matrices in the objective function when there are no active constraints. In this paper, for simplicity, we choose the estimated spatial bandwidth as the spatial benchmark, which can be approximated from the spatial response width.

For the spatial bandwidth, the mathematical operators separating the spatially controllable and uncontrollable components $\mathbb{P}_{c,user}$ and $\mathbb{P}_{u,user}$ are constructed as,

$$\mathbb{P}_{c,user} = P_c^T P_c, \quad \mathbb{P}_{u,user} = I - P_c^T P_c, \tag{26}$$

where $P_c = [P(1:r,:)\ \ 0\ \ P(m-r+2:m,:)]$[1], P is the m-dimensional Fourier matrix and in Matlab it can be defined as $P = fft(eye(m))/sqrt(m)$. r is the selected spatial bandwidth. ***Notice that the selection of P will affect the performance index but this effect will be so small that the decision (e.g. as to the presence or not of MPM) based on the performance index will not be influenced. Choosing P as the Fourier matrix is for the sake of being consistent with the definition of spatial bandwidth which is used in the tuning of CD controllers and expressed in the frequency domain. Moreover, it is more intuitive for the users to specify the desired spatial bandwidth by choosing the Fourier matrix.*** According to the rule-of-thumb proposed in [37], r can be determined directly with the knowledge of spatial response width. The spatially controllable components, for both residual and steady-state profile, are

$$y_{ss,user} = \mathbb{P}_{c,user} y_{ss},\ y_{r,user}(t) = \mathbb{P}_{c,user} y_r(t). \tag{27}$$

In the temporal direction, when the implemented controller is not MVC, the controllable (either from (22) or (26)) residual profile $y_{r,c}(t)$ can be expressed as the impulse response form,

$$\begin{aligned} y_{r,c}(t) \quad = \quad & f_0 e_c(t) + f_1 e_c(t-1) + \ldots + f_{d-1} e_c(t-d+1) + \\ & f_d e_c(t-d) + f_{d+1} e_c(t-d-1) + \ldots . \end{aligned} \tag{28}$$

For the temporal MVC, there will be no terms remaining after the first d terms in the time series model (28). The temporal user-specified term (scalar) $G_R(z^{-1})$ can be used to define a desirable form for the remaining terms such that,

$$y_{r,c}(t) = f_0 e_c(t) + \ldots + f_{d-1} e_c(t-d+1) + G_R(z^{-1}) e_c(t-d). \tag{29}$$

The user-specified term $G_R(z^{-1})$ can be selected as [14],

$$G_R(z^{-1}) = \left[1 - G_F(z^{-1})\right] R(z^{-1}), \tag{30}$$

where $G_F(z^{-1})$ is the desired complementary sensitivity function with the first order form,

$$G_F(z^{-1}) = \frac{1-\alpha_R}{1-\alpha_R z^{-1}}, \tag{31}$$

and α_R is the calculated via the desired closed-loop time constant τ_{des},

$$\alpha_R = e^{-\frac{T_s}{\tau_{des}}}, \tag{32}$$

where T_s is the sampling time. $R(z^{-1})$ is from the dynamic part of the disturbance model (5) via the Diophantine decomposition (12), $R(z^{-1}) = H(z^{-1})/A(z^{-1})$. By combining the spatial user-specified controllable and uncontrollable operators (27) and the temporal user-specified term (30), the user-specified counterpart of η_2 can be obtained as follows,

$$\eta_{2,user} = \frac{trace\left[\sum_{i=0}^{d-1} F_i \Sigma_{e_{user}} F_i^T + \Sigma_{user}\right]}{trace(\Sigma_{y_{user,mse}})}, \tag{33}$$

[1]Note that the colon follows Matlab's notation. $P(1:r,:)$ represents the first r columns of P, and $P(m-r+2:m,:)$ represents the last $r-1$ columns of P.

where $\Sigma_{e_{user}} = \mathbb{E}[e_{user}(t)e_{user}^T(t)]$, $e_{user}(t) = \mathbb{P}_{c,user}e(t)$, $\Sigma_{user} = Var[G_R(z^{-1})e_{user}(t)]$. The denominator of $\eta_{2,user}$ is,

$$\Sigma_{y_{user,mse}} = \Sigma_{y_{r,user}} + diag(y_{ss,user}y_{ss,user}^T), \tag{34}$$

where $\Sigma_{y_{r,user}} = \mathbb{E}[y_{r,user}(t)y_{r,user}^T(t)]$. It can be seen that compared with the MVC benchmark η_2, in the spatial direction, the only difference of $\eta_{2,user}$ is that the controllable projector is replaced by a user-specified projector $\mathbb{P}_{c,user}$, which is applied to both steady-state and residual profiles. In the temporal direction, an additional term $G_R(z^{-1})$ which represents the desirable sensitivity function is included into the residual benchmark. Note that this term is not applicable to the steady-state profile since there are no dynamics (or time-delay performance limitation) for the steady-state profile.

Remark 4: Note that (30) implies that in order to obtain the user-specified benchmark, the disturbance model has to be available, which is not realistic as the disturbance model may change from time to time. However, for simplicity, we assume the disturbance model is known in this paper. This assumption is valid since there have been extensive methods proposed on the identification of disturbance models using closed-loop input-output data [24], [25].

Remark 5: ***If the user-specified term is selected to be the same as the nominal closed-loop response (when the tuning parameters of the controller are available), then the highest achievable user-specified performance index will be one. In this case, the value of the user-specified performance index will make more sense and provide better indication of the control performance.***

V. Performance Monitoring

In order to compute the previous performance indices, the residual profile has to be fitted into a moving average model (refer to (21) and (28)) to obtain the estimates of the impulse response coefficient matrices and the white noise covariance. However, due to the high input-output dimensions of the CD processes, the computational burden plays an essential role in the multivariate time series estimation. In this section, a novel technique is proposed to reduce the computations in the performance monitoring.

A. Vector Autoregressive Modeling

As illustrated in previous sections, to proceed with performance monitoring, we need to perform the following multivariate time series identification,

$$y_r(t) = \Theta_1 y_r(t-1) + \ldots + \Theta_p y_r(t-p) + e(t), \tag{35}$$

where $e(t) \in \mathbb{R}^m$ is the white noise vector. The $\Theta_i \in \mathbb{R}^{m\times m}$, $i = 1,2,\ldots,p$, are the coefficient matrices to be estimated for the vector autoregressive (VAR) process, where p is the temporal order selected by the user. If Θ_i, $i = 1,2,\ldots,p$, are chosen to be full matrices, the estimation of the VAR model will be computationally expensive. However, we can assume that Θ_i, $i = 1,2,\ldots,p$, are Toeplitz-structured, because in industry most CD controllers have limited spatial response width, which means that the CD multivariate controller will be band-diagonal [28]–[30]. Furthermore, the plant G in general is Toeplitz-structured, and as a result the closed-loop sensitivity function will be approximately band-diagonal [27]. By taking advantage of the special structure of Θ_i, the estimation problem can be greatly simplified through the basis matrices method described below.

We construct basis matrices to decompose each Toeplitz-structured coefficient as the sum of a series of scalars multiplied by simple basis matrices. Each Toeplitz-structured VAR coefficient Θ_i matrix has the form,

$$\begin{aligned}\Theta_i &= \text{toeplitz}\{\theta_{i,1},\ldots,\theta_{i,q},\ldots\}_{m\times m}\\ &= \begin{bmatrix} \theta_{i,1} & \theta_{i,2} & \ldots & \theta_{i,q} & & & & & \\ \theta_{i,2} & \theta_{i,1} & \theta_{i,2} & \ldots & \theta_{i,q} & & & & \\ \vdots & \ddots & \ddots & \ddots & \vdots & \ddots & & & \\ \theta_{i,q} & \ldots & \theta_{i,2} & \theta_{i,1} & \theta_{i,2} & \ldots & \theta_{i,q} & & \\ & \ddots & \ddots & \ddots & \ddots & \ddots & \ddots & \ddots & \\ & & \theta_{i,q} & \ldots & \theta_{i,2} & \theta_{i,1} & \theta_{i,2} & \ldots & \theta_{i,q} \\ & & & \ddots & \vdots & \ddots & \ddots & \ddots & \vdots \\ & & & & \theta_{i,q} & \ldots & \theta_{i,2} & \theta_{i,1} & \theta_{i,2} \\ & & & & & \theta_{i,q} & \ldots & \theta_{i,2} & \theta_{i,1} \end{bmatrix}\end{aligned} \tag{36}$$

where q is the spatial order selected by the user. There are only q unknown scalars to be estimated in each coefficient matrix. The unknown scalars $\theta_{i,j}, j = 1,\ldots,q$, are extracted from Θ_i by rewriting the large dimensional matrix as the sum of simple terms,

$$\Theta_i = \sum_{j=1}^{q} \theta_{i,j}E_j, \tag{37}$$

where $E_j, j = 1,\ldots,q$ are basis matrices with the j^{th} super-diagonal and $-j^{th}$ subdiagonal entries as ones, while the other entries are all zeros. For example, the basis matrix for the case $m = 6, j = 3$, is

$$E_3 = \begin{bmatrix} 0 & 0 & 1 & 0 & 0 & 0 \\ 0 & 0 & 0 & 1 & 0 & 0 \\ 1 & 0 & 0 & 0 & 1 & 0 \\ 0 & 1 & 0 & 0 & 0 & 1 \\ 0 & 0 & 1 & 0 & 0 & 0 \\ 0 & 0 & 0 & 1 & 0 & 0 \end{bmatrix}. \tag{38}$$

Thus the i-th term of the VAR model (35) can be written as,

$$\begin{aligned}\Theta_i y_r(t-i) &= \sum_{j=1}^{q} \theta_{i,j}E_j y_r(t-i)\\ &= \sum_{j=1}^{q} \theta_{i,j}\tilde{y}_{r,ij}(t-i),\end{aligned} \tag{39}$$

where $\tilde{y}_{r,ij}(t-i) = E_j y_r(t-i)$. The overall VAR model becomes

$$\begin{aligned} y_r(t) &= \theta_{11}\tilde{y}_{r,11}(t-1) + \ldots + \theta_{1q}\tilde{y}_{r,1q}(t-1)\\ &\quad + \theta_{21}\tilde{y}_{r,21}(t-2) + \ldots + \theta_{2q}\tilde{y}_{r,2q}(t-2)\\ &\quad \ldots\\ &\quad + \theta_{p1}\tilde{y}_{r,p1}(t-p) + \ldots + \theta_{pq}\tilde{y}_{r,pq}(t-p)\\ &\quad + e(t)\\ &\triangleq \tilde{Y}_r(t-1)\theta + e(t),\end{aligned} \tag{40}$$

where

$$\tilde{Y}_r(t-1) = \begin{bmatrix} \tilde{y}_{r,11}(t-1) & \tilde{y}_{r,12}(t-1) & \dots & \tilde{y}_{r,pq}(t-p) \end{bmatrix},$$
$$\theta = \begin{bmatrix} \theta_{11} & \theta_{12} & \dots & \theta_{pq} \end{bmatrix}^T.$$

The following steps for identification are similar to the scalar autoregressive model identification. There are various well-developed techniques for this problem, e.g., the least squares method. The residuals $\hat{e}(t)$ resulting from the identification are considered to be estimates of the innovations $e(t)$. The estimate of the coefficients θ is denoted as $\hat{\theta}$. Then the Toeplitz coefficients $\hat{\Theta}_i, i = 1,\dots,p$, can be determined by reconstructing $\hat{\theta}$. By using the basis matrices, the estimation of the VAR model (35) can be significantly simplified.

In order to calculate the performance indices, the VAR model above is transformed into the following vector moving average (VMA) model by using the technique in [26],

$$y_r(t) = \hat{\Phi}_0\hat{e}(t) + \dots + \hat{\Phi}_{d-1}\hat{e}(t-d+1) + \hat{\Phi}_d\hat{e}(t-d) + \dots, \tag{41}$$

where

$$\hat{\Phi}_0 = I, \tag{42}$$
$$\hat{\Phi}_i = \sum_{j=1}^{i} \hat{\Phi}_{i-j}\hat{\Theta}_j, \quad i = 1,\dots,d,\dots. \tag{43}$$

Although the order of the VMA model (41) will be infinite, we are only interested in the first d terms since they are the coefficients required in evaluating the benchmark. ***When applying this algorithm, d can be selected to be the time delay in the model as an approximation of the true time delay in the process.*** On the other hand, due to the spatial performance limitation resulting from the structure of the transfer matrix G, only the controllable components of the estimated residuals $\hat{e}_c(t)$ and the output profile $y_{r,c}(t)$ are considered. The covariance matrix of the output under temporal MVC and within the column space of G matrix is thus expressed as,

$$\hat{\Sigma}_{mv} = \sum_{i=0}^{d-1} \hat{\Phi}_i \Sigma_{\hat{e}_c} \hat{\Phi}_i^T, \tag{44}$$

where $\Sigma_{\hat{e}_c} = \mathbb{E}[\hat{e}_c(t)\hat{e}_c^T(t)]$ is the covariance of the controllable residual, $\hat{e}_c(t)$. The overall estimated performance index $\hat{\eta}_2$ is obtained as,

$$\hat{\eta}_2 = \frac{trace(\hat{\Sigma}_{mv})}{trace(\Sigma_{y_{c,mse}})}, \tag{45}$$

where $\hat{\eta}_2$ is the estimate of the performance index η_2.

B. Performance Monitoring Algorithm

As illustrated in the previous sections, any given CD data set (without MD variations) can be separated into steady-state profile and residual profile. The steady-state profile is obtained by averaging the data for each CD bin over all scans. In order to calculate the performance indices (19), (24) or (33), the steady-state profile y_{ss} has to be separated into controllable parts $y_{ss,c}$ and uncontrollable parts $y_{ss,u}$ according to the column space of G or the spatial bandwidth. A VAR model (35) is applied to the residual profile $y_r(t)$ to obtain the controller-invariant variation due to time-delay and spatial bandwidth limitations. The uncontrollable parts of the steady-state variation, $y_{ss,u}$, and the controller-invariant variations of the residuals, $y_{r,u}$, are combined to obtain the overall benchmark in (19). The algorithm we propose to calculate (24) is as follows:

1. For a given data set, Y, ensure the mean value of each scan is zero (i.e., no MD variation).
2. Calculate the average CD profile by averaging the data set across all scans, record it as y_{ss}. Remove the mean of each CD bin to obtain the residual profile $y_r(t)$.
3. Perform Toeplitz-structure VAR estimation (35) using the residual profile $y_r(t)$ with the selected spatial order q and temporal order p. Ensure the whiteness of the white noise estimate $\hat{e}(t)$.
4. Transform the VAR model into a VMA model (41) and obtain the coefficient matrices $\hat{\Phi}_i, i = 0,\dots,d-1$.
5. Construct the operator $\mathbb{P}_c$ based on the column space (22), and get the following controllable components: $\hat{e}_c = \mathbb{P}_c\hat{e}(t)$, $y_{r,c} = \mathbb{P}_c y_r$, $y_{ss,c} = \mathbb{P}_c y_{ss,c}$.
6. Calculate the estimated minimum covariance $\hat{\Sigma}_{mv}$ in (44) and $\Sigma_{y_{c,mse}}$ in (45).
7. Obtain the estimated performance index from (45).

For the user-specified benchmark $\eta_{2,user}$, in Step 5, the operator $\mathbb{P}_c$ can be constructed based on the selected spatial bandwidth (26). Besides, the temporal user-specified term can be obtained from the knowledge of the desired closed-loop time constant together with (30) and (32).

Remark 6: In order to obtain the performance index, one has to fit the CD profile to the VAR model (35), which requires each output channel to be zero meaned. Otherwise, there will be an offset term showing up in (35), as illustrated in [26]. This fact motivates the profile partition in Section II and III. After splitting the output measurements into steady-state profile and residual profile, we can simply fit only the residual profile into (35).

VI. Examples

It has been mentioned that various factors such as poorly tuned controller, model-plant mismatch, change of disturbance dynamics, etc., can cause a drop in the performance index. From the perspective of industry engineers, when the model quality deteriorates, a new model has to be identified from identification experiments. Therefore, it is of interest to find whether the proposed performance benchmarks are sensitive to model-plant mismatches. In this section, the validity of the proposed performance benchmark for the CD process is tested by data sets from both paper machine simulators and paper mills. For simplicity, we only consider the case of controlling a single paper property using a single actuator array.

A. Simulation Results

In this subsection, scenarios with various types of model-plant mismatches are created to test the sensitivity of the performance index. In this simulation, the employed control strategy is the two-dimensional loopshaping technique. The number of actuators in the array of the CD is 238, and the number of CD bins downstream at the scanner side is 714.

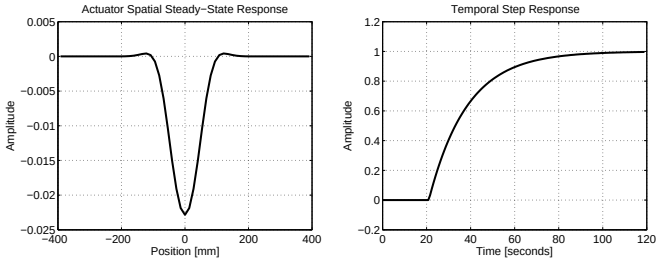

Fig. 3. Spatial impulse steady-state response and the temporal step response of a single actuator. The negative peak of the spatial response is due to the negative gain of the actuator spatial model.

The continuous steady-state spatial response shape of a single actuator is determined by the four parameters, gain γ, width ξ, divergence β and attenuation α (see [38] for more details). In the temporal direction, the actuator dynamic model $g(s)$ is assumed to be first-order plus time-delay with unit steady-state gain,

$$g(s) = \frac{1}{\tau s + 1} e^{-\tau_d s}, \tag{46}$$

where τ the time constant τ and τ_d is the time delay τ_d. In the simulator, the nominal values of these parameters on both the plant and the process model are set initially as $\gamma_0 = -0.03, \xi_0 = 164mm, \beta_0 = 0.15, \alpha_0 = 7.0, \tau_0 = 17.34s, \tau_{d0} = 21s$. Figure 3 illustrates the spatial steady-state impulse response and the temporal step response of one actuator with these nominal parameter values. This process is relatively easy to control since there are no negative side lobes in the spatial response shape. The controllers are properly tuned by using the two-dimensional loop shaping technique based on the nominal process model.

In order to investigate the sensitivity of the proposed performance index in detecting the model-plant parametric mismatch, scenarios with different levels of mismatch for these spatial and temporal parameters are created. For convenience, we manually increase and decrease the parameter values of the plant while the parameter values of the process model used by the controller remain unchanged. In the following simulations, we denote $\gamma, \xi, \beta, \alpha, \tau, \tau_d$ without subscripts as the parameter values in the plant. In addition, positive mismatches indicate that the value of the parameter in the plant is greater than the corresponding value in the model. For instance, positive gain mismatch means the gain of the plant is greater than the gain of the model used by the controller.

Figures 4-7 illustrate the simulation results with respect to various levels of parametric mismatch for each parameter in the spatial model of the actuator. Note that in this simulation, the sampling time is 20 seconds and the data is selected after the initial transient behavior has been settled down. The number of scans in the selected portion of the data is 500. The left-hand-side graph in each figure shows the comparison between the spatial response shape of each mismatched plant with that of the nominal case, from which we can know the significance of the distortion the corresponding parametric mismatch can cause in the spatial response shape. The graph on the right-hand-side of each figure shows the corresponding

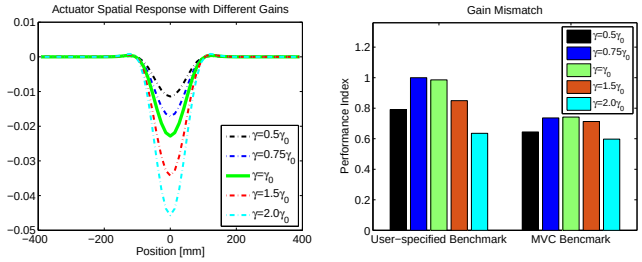

Fig. 4. Performance indices for different levels of gain mismatch. Both the user-specified benchmark and MVC benchmark are tested. Note that γ_0 is the nominal gain value used by the controller, γ is the actual gain value of the process plant.

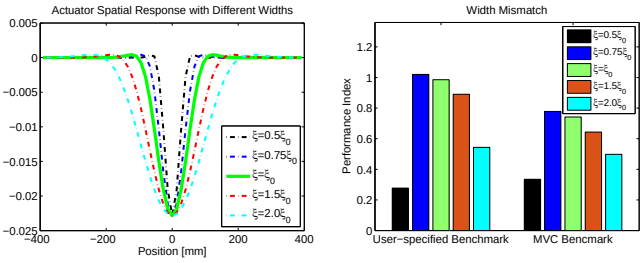

Fig. 5. Performance indices for different levels of width mismatch. Both the user-specified benchmark and MVC benchmark are tested. Note that ξ_0 is the nominal width value used by the controller, ξ is the actual width value of the process plant.

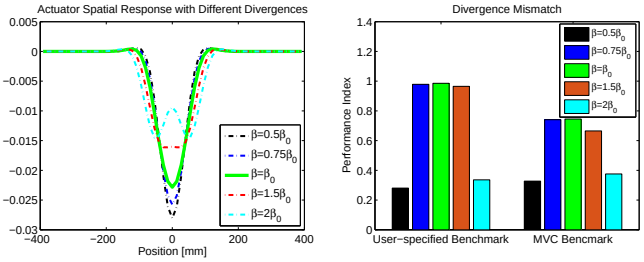

Fig. 6. Performance indices for different levels of divergence mismatch. Both the user-specified benchmark and MVC benchmark are tested. Note that β_0 is the nominal divergence value used by the controller, β is the actual divergence value of the process plant.

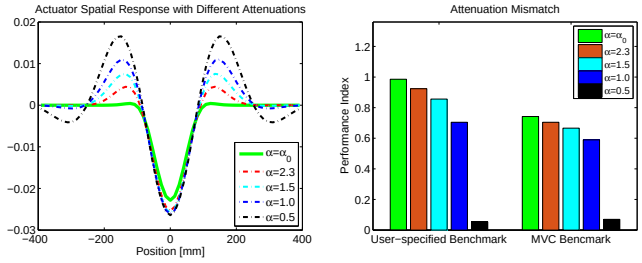

Fig. 7. Performance indices for different levels of attenuation mismatch. Both the user-specified benchmark and MVC benchmark are tested. Note that α_0 is the nominal attenuation value used by the controller, α is the actual attenuation value of the process plant. The four mismatched attenuation values are practical scenarios in the industry.

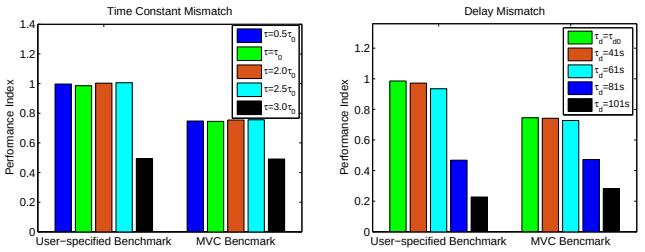

Fig. 8. Performance indices for different levels of time constant and time delay mismatch. Both the user-specified benchmark and MVC benchmark are tested. Note that τ_0 and τ_{d0} are the nominal time constant and time delay value used by the controller, τ and τ_d are the actual time constant and time delay value of the process plant.

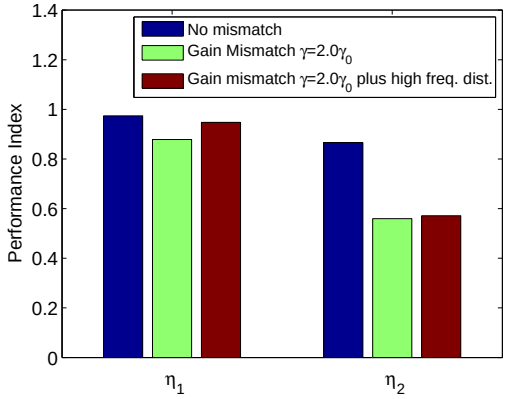

Fig. 9. Comparison of performance index η_1 and η_2 with high frequency spatial disturbance

calculated performance index for each case based on both MVC benchmark η_2 and user-specified benchmark $\eta_{2,user}$. One can see that in general the user-specified performance indices are higher than the MVC benchmark, which agrees well with the previous analysis as the user-specified benchmark is more practical and less aggressive. These figures show that for most cases of MPM, the performance indices based on both the MVC benchmark and user-specified benchmark decrease as the degree of MPM increases. However, the performance indices of gain mismatch and width mismatch with $\gamma = 0.75\gamma_0$ and $\xi = 0.75\xi_0$ show better performance than the no MPM case. It can be explained that the degree of mismatch is not severe and within the tolerance of the implemented robust controller and in these cases the true process is more close to the model compared with the nominal case. However, for the cases with large mismatches, all the performance indices drop. Besides, the performance index is sensitive to the divergence mismatch but not so sensitive to the attenuation mismatch. Figure 8 shows the performance indices for the time constant and time delay mismatches. One can see that the performance indices are able to detect the drop in performance due to the time constant or delay mismatch as well, but not so sensitive as the spatial parameters. Note that for some cases (e.g. width mismatch with $\xi = 0.75\xi_0$), the indices show a slightly better performance compared with the nominal case. Table I shows the partitioned variances for each simulated case, in which σ_T, σ_{CD}, σ_{Res} refer to the total variance, CD variance (variance of the steady-state profile) and residual variance. Note that there is no MD variance since the MD profile has been removed beforehand. By comparing these results with the previous performance indices one can see, mostly, the larger variance in either CD or residual than the nominal case will correspond to worse control performance. Therefore we can conclude that the proposed performance indices are not only affected by the CD variance, but also the residual variance.

To demonstrate the advantage of the performance index η_2 over η_1, another simulation is carried out with gain mismatch $\gamma = 2.0\gamma_0$ and a spatial sinusoidal disturbance (with frequency greater than the closed-loop spatial bandwidth) added to the output. The performance index is expected to drop relative to the normal case due to the presence of gain mismatch, however, it is desirable for the high frequency spatial disturbance to affect the index as little as possible. The simulation results under this situation are illustrated in Figure 9. The performance index η_1 with both positive gain mismatch and high frequency spatial disturbance remains almost the same as the normal case, while it drops a little for the case with gain mismatch only. Thus it is not straightforward to observe the performance deterioration in the presence of high frequency spatial disturbance if we are using performance index η_1. However, for performance index η_2, the presence of high frequency spatial disturbance has almost no affect, and the drop in the performance index is due to the gain mismatch. Moreover, one may find from ***Figure 9*** that the performance index η_1 is not so sensitive to the mismatch as the index η_2 since the drop due to gain mismatch is much smaller compared with η_2. Therefore, we can achieve reliable assessment based on performance index η_2. As mentioned in the previous section, the misleading conclusion from η_1 is a result of the energy of the deterministic high frequency disturbance inflating both the covariance of the benchmark and the actual output in (19). The ratio between the two covariance matrices will be very close to one.

B. Industrial Example

In this subsection, data sets from a paper mill are used to validate the effectiveness of the proposed techniques. The number of actuators and CD bins in this example are 114 and 402, respectively. Figure 10a illustrates the measured profile of the dry weight without MD variations. Note that the edges of the profile that were not controlled have been removed. Figure 10b shows the corresponding actuator profile with lower bound 10 and upper bound 90. The sampling interval is 16 seconds and the number of scans is 551. The implemented controller is a multivariate CD-MPC. Performance monitoring with a moving window of size 200 scans is applied to the measured output profile, and the corresponding performance indices in terms of the time is demonstrated in Figure 11a. Both the user-specified benchmark ($\eta_{2,user}$ in the blue solid line) and the MVC benchmark (η_2 in the red dash-dotted line and η_1 in the black dashed line) are used in the calculation of these performance indices. ***The VMA model in the algorithm proposed in Section V is estimated repeatedly for each***

TABLE I
VARIANCE PARTITION FOR EACH SIMULATED CASE

γ MPM	σ_T	σ_{CD}	σ_{Res}	ξ MPM	σ_T	σ_{CD}	σ_{Res}	β MPM	σ_T	σ_{CD}	σ_{Res}
$\gamma = 0.50\gamma_0$	0.2575	0.0687	0.1888	$\xi = 0.50\xi_0$	0.3715	0.1812	0.1903	$\beta = 0.50\beta_0$	0.3804	0.1861	0.1943
$\gamma = 0.75\gamma_0$	0.2454	0.0523	0.1930	$\xi = 0.75\xi_0$	0.2391	0.0453	0.1937	$\beta = 0.75\beta_0$	0.2434	0.0459	0.1975
$\gamma = 1.50\gamma_0$	0.2511	0.0453	0.2059	$\xi = 1.50\xi_0$	0.2621	0.0643	0.1979	$\beta = 1.50\beta_0$	0.2571	0.0459	0.1975
$\gamma = 2.00\gamma_0$	0.2739	0.0485	0.2253	$\xi = 2.00\xi_0$	0.2979	0.1017	0.1961	$\beta = 2.00\beta_0$	0.3497	0.1579	0.1918
α MPM	σ_T	σ_{CD}	σ_{Res}	τ MPM	σ_T	σ_{CD}	σ_{Res}	τ_d MPM	σ_T	σ_{CD}	σ_{Res}
$\alpha = 2.3$	0.2496	0.0505	0.1991	$\tau = 0.5\tau_0$	0.2428	0.0480	0.1948	$\tau_d = 41$	0.2448	0.0473	0.1976
$\alpha = 1.5$	0.2595	0.0543	0.2052	$\tau = 2.0\tau_0$	0.2406	0.0472	0.1933	$\tau_d = 61$	0.2480	0.0491	0.1989
$\alpha = 1.0$	0.2756	0.0594	0.2162	$\tau = 2.5\tau_0$	0.2447	0.0480	0.1967	$\tau_d = 81$	0.3093	0.1060	0.2033
$\alpha = 0.5$	1.8128	0.2307	1.5758	$\tau = 3.0\tau_0$	0.3007	0.1059	0.1948	$\tau_d = 101$	0.4271	0.2224	0.2047

Note: For the normal case, $\sigma_T = 0.2439$, $\sigma_{CD} = 0.0476$, $\sigma_{Res} = 0.1962$.

window in order to the compute those performance indices. For each window, on average, it takes only 1.68 seconds to identify the VMA model, which is much less than the sampling interval and thus fast enough for the online monitoring. Note that there are no performance indices for the first few scans since they are calculated only after the 200th scan. It can be observed that all these performance indices show consistent patterns except their levels. The performance index η_2 shows the worst performance since it is based on the aggressive MVC benchmark. The high level of η_1 is due to that the spatially uncontrollable components in the denominator and numerator of (19) are the majority. The user-specified benchmark $\eta_{2,user}$ also shows higher performance index than η_2, which makes sense since $\eta_{2,user}$ is based on a more practical and less aggressive benchmark.

For this industrial example, the user-specified benchmark is specified based on the implemented controller. Thus good control performance is expected to have $\eta_{2,user}$ close to one (see Remark 5). However, from Figure 11a we find that all these performance indices are less than 0.7, which is not satisfactory. In order to investigate the root causes of the low performance, we generated the steady-state profile of both the dry weight and the actuator as well as the power spectrum of the averaged dry weight profile, which are shown in Figure 11b-d. From the spectrum plot, it is obvious that some low frequency components are left in the controllable range which contributes to the poor performance. These low frequency components are due to the large fluctuations of the dry weight profile in the first 60 bins and those around the 280th bin. From the averaged actuator profile, we find that the actuator saturations in the first few zones and around the 85th zone explain the reason that those fluctuations in the output profile were not rejected. Therefore, the actuator saturation is one root cause of the low performance index. However, further diagnosis or data pre-processing techniques are required to know if the model-plant mismatch is also one of the root causes. For instance, in order to reduce the false positives on the model-plant mismatch diagnosis, we may select a portion of the data set in which there are no severe actuator saturations, irregular disturbances or poorly tuned control to apply the performance monitoring algorithm.

It should be pointed out that the computational speed of the performance index is an important concern for the online performance monitoring. For the simulator example and the industrial example studied in this work, the computation speed is fast enough (less than 3 seconds for each window), compared with the sampling interval (more than 15 seconds for most paper machines). Thus the proposed algorithms for computing the performance indices are efficient enough for online performance monitoring.

VII. SUMMARY

In this paper, the spatial and temporal MVC benchmark for both the steady-state profile and the residual profile are analyzed for the CD process of paper machines. Performance indices are proposed based on the steady-state and residual MVC benchmark. The sensitivity of these performance indices with respect to large spatial high-freqency disturbances are analyzed and compared. Furthermore, the corresponding user-specified benchmark is put forward by taking into account the desirable closed-loop dynamics in both temporal and spatial directions. A novel technique is employed to improve the efficiency of computations associated with the multivariate time series model identification. The idea of this technique is to decompose the coefficient matrices into a series of simple multiplications between scalars and basis matrices. The basis matrices are constructed based on the special structure of the coefficient matrices. Data sets from a CD simulator are used to test the sensitivity of the proposed performance indices with respect to various types of mismatch existing in the CD process as well as to the spatial high-frequency disturbances. Finally, an industrial data set is introduced to test the effectiveness of the proposed performance monitoring technique.

APPENDIX A
VARIANCE PARTITION

For the measured two-dimensional data set $Y \in \mathbb{R}^{m\times N}$, it has the following structure:

$$Y = \begin{array}{c} \\ 1 \\ \vdots \\ i \\ \vdots \\ m \end{array} \begin{array}{c} \begin{array}{cccccc} 1 & \cdots & j & \cdots & N \end{array} \\ \begin{bmatrix} y_{11} & \cdots & y_{1j} & \cdots & y_{1N} \\ \vdots & \ddots & \vdots & \ddots & \vdots \\ y_{i1} & \cdots & y_{ij} & \cdots & y_{iN} \\ \vdots & \ddots & \vdots & \ddots & \vdots \\ y_{m1} & \cdots & y_{mj} & \cdots & y_{mN} \end{bmatrix} \end{array}, \tag{47}$$

where each row of Y refers to the N measurements of one data box, while each column of Y represents the measured profile at

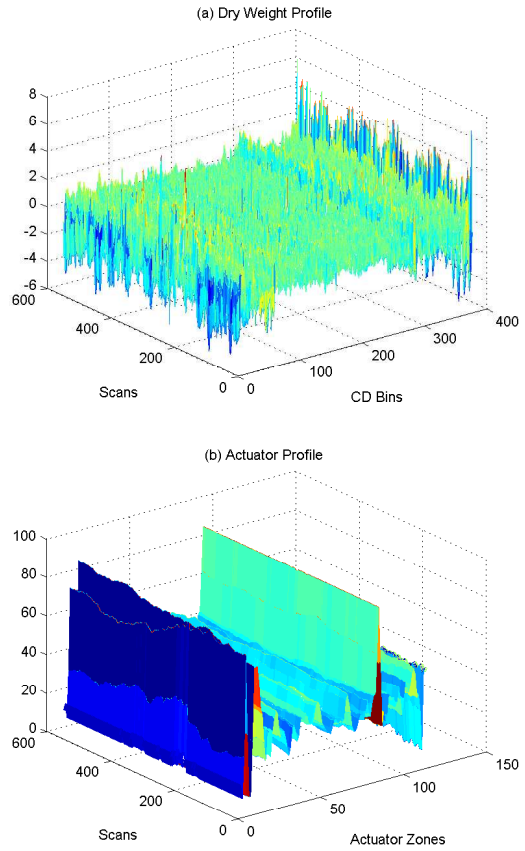

Fig. 10. Three-dimensional plot of the profile from industrial data set. (a): The dry weight profile with 376 measurement bins; (b): The actuator profile with 114 actuator zones.

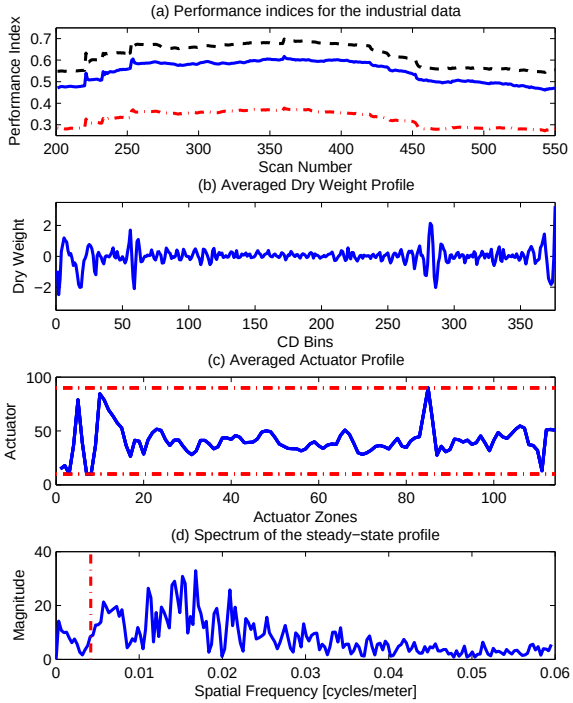

Fig. 11. The analysis of the industrial data. (a): The moving window performance indices for the measured data. Blue solid line: $\eta_{2,user}$; Red dash-dotted line: η_2; Black dashed line: η_1; (b): The steady-state of the entire dry weight profile; (c): The steady-state of the entire actuator profile with lower bound and upper bound (red dash-dotted line); (d): The spectrum of the averaged dry weight profile and the approximated spatial bandwidth (red dash-dotted line).

each scan across all the data boxes. The overall sample mean of the data set Y is defined as,

$$\bar{Y} = \sum_{i=1}^{m}\sum_{j=1}^{N}\frac{y_{ij}}{Nm}. \tag{48}$$

The total sample variance σ_T^2 can be calculated as,

$$\sigma_T^2 = \sum_{i=1}^{m}\sum_{j=1}^{N}\frac{(y_{ij}-\bar{Y})^2}{Nm-1}. \tag{49}$$

The CD sample variance σ_{CD}^2 can be calculated as,

$$\sigma_{CD}^2 = \sum_{i=1}^{m}\frac{(\tilde{Y}_i-\bar{Y})^2}{m-1}, \tag{50}$$

where $\tilde{Y}_i = \sum_{j=1}^{N}\frac{y_{ij}}{N}$. The MD sample variance σ_{MD}^2 can be calculated as,

$$\sigma_{MD}^2 = \sum_{j=1}^{N}\frac{(\tilde{Y}_j-\bar{Y})^2}{N-1}, \tag{51}$$

where $\tilde{Y}_j = \sum_{i=1}^{m}\frac{y_{ij}}{m}$. The residual sample variance σ_{Res}^2 is calculated as,

$$\sigma_{Res}^2 = \sigma_T^2 - \sigma_{CD}^2 - \sigma_{MD}^2. \tag{52}$$

REFERENCES

[1] R.M. Morales and W.P. Heath, "The robustness and design of cross-directional control via integral quadratic constraints," *IEEE Transactions on Control System Technology*, vol. 19, no. 6, pp. 1421–1432, 2011.

[2] T. Maenpaa. *Robust Model Predictive Control for Cross-Directional Processes*. PhD Thesis, Helsinki University of Technology, Finland, 2006.

[3] W.P. Heath, "Orthogonal functions for cross-directional control of web forming processes," *Automatica*, vol. 32, no. 2, pp. 183–198, 1996.

[4] K. Kristinnson and G.A. Dumont, "Cross-directional control on paper machines using gram polynomials," *Automatica*, vol. 32, no. 4, pp. 533–548, 1996.

[5] P. Lundstrom, S. Skogestad, and J.C. Doyle, "Two-degree-of-freedom controller design for an ill-conditioned distillation process using μ-synthesis," *IEEE Transactions on Control System Technology*, vol. 7, no. 1, pp. 12–21, 1999.

[6] S. Skogestad, M. Morari, and J.C. Doyle, "Robust control of ill-conditioned plants: High-purity distillation," *IEEE Transactions on Automatic Control*, vol. 33, no. 12, pp. 1092–1105, 1988.

[7] A. Rigopoulos and Y. Arkun, "Reduced order cross-directional controller design for sheet forming processes," *IEEE Transactions on Control System Technology*, vol. 11, no. 5, pp. 746–756, 2003.

[8] D. Gorinevsky, R. Vyse, and M. Heaven, "Performance analysis of cross-direction process control using multivariable and spectral models," *IEEE Transactions on Control System Technology*, vol. 8, no. 4, pp. 589–600, 2000.

[9] A.P. Featherstone, J.G. VanAntwerp, and R.D. Braatz. *Identification and Control of Sheet and Film Processes*. London: Springer, 2000.

[10] T.J. Harris, "Assessment of control loop performance," *The Canadian Journal of Chemical Engineering*, vol. 467, no. 5, pp. 856–861, 1989.

[11] T.J. Harris, C.T. Seppala, and L.D. Desborough, "A review of performance monitoring and assessment techniques for univariate and multi-

variate control systems," *Journal of Process Control*, vol. 9. no. 1, pp. 1–17, 1999.

[12] T.J. Harris, F. Boudreau, and J.F. MacGregor, "Performance assessment of multivariate feedback controllers," *Automatica*, vol. 32, no. 11, pp. 1505–1518, 1996.

[13] J. Yu and S.J. Qin, "Statistical MIMO controller performance monitoring. Part II: Performance diagnosis," *Journal of Process Control*, vol. 18, no. 3, pp. 297–319, 2008.

[14] B. Huang and S.L. Shah. *Performance Assessment of Control Loops: Theory and Applications*. Berlin: Springer, 1999.

[15] C. Liu, B. Huang, and Q. Wang, "Control performance assessment subject to multi-objective user-specified performance characteristics," *IEEE Transactions on Control Systems Technology*, vol. 19, no. 3, pp. 682–691, 2011.

[16] A.S. Badwe, R.S. Patwardhan, S.L. Shah, S.C. Patwardhan, and R.D. Gudi, "Quantifying the impact of model-plant mismatch on controller performance," *Journal of Process Control*, vol. 20, no. 4, pp. 408–425, 2010.

[17] A.R. Taylor and S.R. Duncan, "Bayesian methods for control loop performance assessment in cross-directional control," In *Proceeding of the* 16^{th} *IFAC World Congress*, Czech Republic, vol. 16, no. 1, pp. 1478–1483, 2005.

[18] S.R. Duncan, G.A. Dumont, and D.M. Gorinevsky, "Evaluating the performance of cross-directional control systems," In *Proceedings of the American Control Conference*, San Diego, California, pp. 3092–3096, 1999.

[19] S.R. Duncan, G.A. Dumont, and D.M. Gorinebsky, "Performance monitoring for cross-directional control systems," In *Proceedings of the Control Systems Conference*, Vicotria, Canada, pp. 173–177, 2000.

[20] R.S. Patwardhan and S.L. Shah, "Issues in performance diagnostics of model-based controllers," *Journal of Process Control*, vol. 12, no. 3, pp. 413–427, 2002.

[21] A.S. Badwe, R.D. Gudi, R.S. Patwardhan, S.L. Shah, and S.C. Patwardhan, "Detection of model-plant mismatch in MPC applications," *Jounral of Process Control*, vol. 19, no. 8, pp. 1305–1313, 2009.

[22] V. Botelho, J.O. Trierweiler, M. Farenzena, and R. Duraiski, "Methodology for detecting modelplant mismatches affecting model predictive control performance," *Industrial & Engineering Chemistry Research*, vol. 54, no. 48, pp. 12072–12085, 2015.

[23] S.R. Duncan and K.W. Corscadden, "Mini-max control of cross-directional variations on a paper machine," In *IEE Proceedings-Control Theory and Applications*, vol. 145, no. 2, pp. 189–195, 1998.

[24] Z. Sun, S. J. Qin, A. Singhal, and L. Megan, "Performance monitoring of model-predictive controllers via model residual assessment," *Journal of Process Control*, vol. 23, no. 4, pp. 473–482, 2013.

[25] Z. Sun, Y. Zhao, and S.J. Qin, "Improving industrial MPC performance with data-driven disturbance modeling," In 50^{th} *IEEE Conference on Decision and Control and European Control Conference*, Orlando, FL, USA, pp. 1922–1927, 2011.

[26] H. Lutkepohl. *New Introduction to Multiple Time Series Analysis*. New York: Springer, 2007.

[27] B. Bamieh, F. Paganini, and M. A. Dahleh, "Distributed control of spatially invariant systems", *IEEE Transactions on Automatic Control*, vol. 47, no. 7, pp. 1091–1107, 2002.

[28] G.E Stewart, D.M. Gorinevsky, and G.A. Dumont, "Feedback controller design for a spatially-distributed system: The paper machine problem," *IEEE Transactions on Control System Technology*, vol. 11, no. 5, pp. 612–628, 2003.

[29] J. Fan, G.E. Stewart, and G.A. Dumont, "Two-dimensional frequency analysis for unconstrained model predictive control of cross-directional processes," *Automatica*, vol. 40, no. 11, pp. 1891–1903, 2004.

[30] D. Gorinevsky, S. Boyd, and G. Stein, "Design of low-bandwidth spatially distributed feedback," *IEEE Transactions on Automatic Control*, vol. 53, no. 1, pp. 257–272, 2008.

[31] M.J. Grimble, "Controller performance benchmarking and tuning using generalized minimum variance control," *Automatica*, vol. 38, no. 22, pp. 2111–2119, 2002.

[32] M. Jelali. *Control Performance Management in Industrial Automation: Assessment, Diagnosis, and Improvement of Control Loop Performance*. London: Springer, 2013.

[33] N. Agarwal, B. Huang, and E.C. Tamayo, "Assessing model prediction control (MPC) performance. 2. Bayesian approach for constraint tuning," *Industrial & Engineering Chemistry Research*, vol. 46, no. 24, pp. 8112–8119, 2007.

[34] A. AlGhazzawi and B. Lennox, "Model predictive control monitoring using multivariate statistics," *Journal of Process Control*, vol. 19, no. 2, pp. 314–327, 2009.

[35] S.R. Duncan. *The Cross-Directional Control of Web Forming Processes*. PhD thesis, University of London, UK, 1989.

[36] O.J. Rojas, G.C. Goodwin, and A. Desbiens, "Study of an adaptive anti-windup strategy for cross-directional control systems," In *Proceedings of the* 41^{st} *IEEE Conference on Decision and Control*, Las Vegas, Nevada, USA, pp. 1331–1336, 2002.

[37] G.E. Stewart, J.U. Backstrom, P. Baker, C. Gheorghe, and R.N. Vyse, "Controllability in cross-directional processes: Practical rules for analysis and design," In *Proceedings of the* 87^{th} *Annual Meeting, PAPTAC*, Montreal, PQ, Canada, pp. C35–C42, 2001.

[38] J. Fan. *Model Predictive Control for Multiple Cross-directional Processes: Analysis, Tuning, and Implementation*. PhD thesis, The University of British Columbia, Canada, 2003.

[39] J.G. VanAntwerp, A.P. Featherstone, R.D. Braatz, and B.A. Ogunnaike, "Cross-directional control of sheet and film processes," *Automatica*, vol. 43, no. 2, pp. 191–211, 2007.

[40] L. Ljung. *System Identification: Theory for the User*. Englewood Cliffs, New Jersey: Prentice-Hall, Inc., 1999.